

Reliable Integrated Space-Oceanic Network Profit Maximization by Bender Decomposition Approach

Sheikh Salman Hassan, Umer Majeed, Choong Seon Hong

Department of Computer Science and Engineering, Kyung Hee University, Yongin, 17104, Republic of Korea

Email: {salman0335, umermajeed, cshong}@khu.ac.kr

Abstract—Maritime network traffic is increasing due to the ongoing need for trade and tourism, thus increasing the demand for convenient, reliable, energy-efficient, and high-speed network access at sea that could be analogous to terrestrial networks. Therefore, to ensure the concept of a connected world under the umbrella of sixth-generation (6G) networks, we propose the next-generation integrated space-oceanic network, which consists of a set of LEO satellites and marine user equipments (MUE). This paper investigates network profit maximization (NPM) by optimizing the MUE association and its resource allocation in downlink communication. The formulated optimization problem corresponds to mixed-integer nonlinear programming (MINLP). To solve this problem, we propose an iterative algorithm based on Bender's decomposition (BD). Numerical results are provided to demonstrate the convergence and effectiveness of our proposed algorithm.

Index Terms—6G, satellite networks, maritime communication, resource allocation, Bender decomposition.

I. INTRODUCTION

The connected world is the agenda of sixth-generation (6G), which needs to ensure worldwide connectivity. Therefore, humans' activities will expand dramatically from space to air, ground, and sea environment in this era. To make sure the worldwide wireless coverage in the 6G networks, it is necessary to integrate marine users equipments (MUE) to form a multi-dimensional space-air-ground-sea network [1]. Moreover, its framework will consider the integration of networks with extremely low latency in wireless connection with super-high throughput demands [1].

Oceanic communication is increasing specifically in video streaming and live surveillance, which poses the demand for ultra-reliable low-latency communication (URLLC). This type of network requirements cannot fulfill with the existing network infrastructure. Moreover, the overall ocean and the marine environment has become one of the new frontiers and the rapidly growing areas of the world's tourism industry. Maritime communication is increasing quickly due to ongoing projects in deep waters, i.e., marine research & life studies, ocean tourism, deep waters drilling platforms, rescue & emergency operations, and offshore aquaculture. The rapid increase in the number of boats, ships, deep-water rigs, vessels

poses a demand for high-level connectivity with low latency and high throughput communication. We can consider several use cases in maritime traffic, which represents a demand for high broadband and narrowband connection such as marine cellular users [2], and maritime internet-of-things (MIoT) [3] respectively. Naval operations, i.e., vessel navigation and surveillance, also pose a demand for URLLC. Moreover, an infotainment requirement of a passenger ship, oil & gas drilling in deep waters, meteorological services in oceans, and emergency rescue operations also need high-level connectivity. All these discussed maritime network applications need rapid and minimal investment for communication.

In the proposed network, the LEO satellites are assumed to be suitable candidates to tackle the maritime network's challenges. The LEO satellite is the most prominent candidate to enable remote location network access where terrestrial access is not available. The LEO satellite can fulfill the quality-of-service (QoS) demands of MUEs due to their mobility and line-of-sight (LOS) nature, which make it suitable in our scenario [4]. The key contributions in this work are summarized as follows,

- We formulate a joint MUE association and resource allocation problem to maximize the network profit in the LEO satellite-based space-oceanic network.
- Our formulated optimization problem is mixed-integer nonlinear programming (MINLP).
- We proposed an iterative algorithm based on Benders decomposition to solve this MINLP.
- Numerical results demonstrate that our proposed algorithm performed well in a given scenario.

The remaining paper is organized as follows. Section II provides related work of 6G and maritime communication, which ensures our network architecture's originality. Section III shows the system model and section IV presents the optimization problem. Section V provides solution based on Bender decomposition. Section VI provides simulation results, and finally section VII concludes this paper.

II. RELATED WORK

Current research on next-generation networks are struggling with the aim of 6G, where the internet of everything (IoE) is looking like a future. Because with the quick improvement of smart edges and rising new applications, e.g., seamless surveillance and monitoring, increment in wireless data and throughput requirement, and current cellular networks, even

This work was supported by the National Research Foundation of Korea (NRF) grant funded by the Korea government (MSIT) (No. 2020R1A4A1018607). *Dr. CS Hong is the corresponding author.

the 5G cannot coordinate with the rapidly increasing network requirements. The 6G dynamic system must cast the high-specialized standards of the new range and effective transmission framework to address up-coming difficulties. The authors sketch the potential necessities and present a review of promising systems' most recent research, developing to 6G [5].

In the existing system, MUE utilizes satellite services or onshore base stations for their communication. International maritime satellite (Inmarsat) is responsible for marine communication, but their data transportation rate is inefficient for time-critical applications [6]. Moreover, to support maritime communication, an offshore base station is also a reliable means of communication. It can prolong the existing fourth (4G) and fifth (5G) generation terrestrial cellular networks to maritime network [7]. Moreover, maritime communication literature covers the network deployments such as [8] presented an overview of the wireless oceanic communication network to affirm the amount of existing sea communication frameworks that withstand the rising communication necessities. Maritime-LTE has also been investigated in [9] for marine users by proposing a scheme with a phased array antenna and user location to the LTE network. However, the maritime communication network is still not well established to provide seamless data connectivity.

III. SYSTEM MODEL

We consider the downlink (DL) wireless communication in a maritime network, as shown in Fig. 1. This network topology has a set $\mathcal{N} = \{1, 2, \dots, N\}$ of floating LEO satellites¹ in space and a set $\mathcal{M} = \{1, 2, \dots, M\}$ of MUEs. Here, we consider the delay insensitive services, i.e., enhanced Mobile Broadband (eMBB) and massive Machine Type Communications (mMTC). Moreover, we assumed each satellite has a backhaul connection with the earth gateway or coastline base station (CBS), depending upon their position. Satellite base stations are deployed to serve MUE, which can be considered boats, fishers, and private yachts. Each Satellite has uniform constellation above the sea surface at the corresponding 3D location denoted as $d_n = (x_n, y_n, h_n), \forall n \in \mathcal{N}$. Similarly, each MUE is deployed randomly in sea region $d_m = (x_m, y_m, h_m)$ within any satellite coverage area. We consider that network topology remains static in the performance observation period. To make the system realistic, we consider that each satellite is already deployed at the desired locations d_n , fulfilling the maritime network demand optimally. We can presume each satellite deployment in maritime networks are according to the given algorithm in [10] at an optimal location in 3D.

A. Channel Model & Link Analysis

A typical composite channel containing both large-scale and small-scale fading is adopted. The communication links work over the Ka-band (26.5-40 GHz) in the considered scenario, a well-defined millimeter wave (mmW) range sufficient for

¹In the rest of paper, the LEO satellite will be considered as a satellite unless otherwise stated.

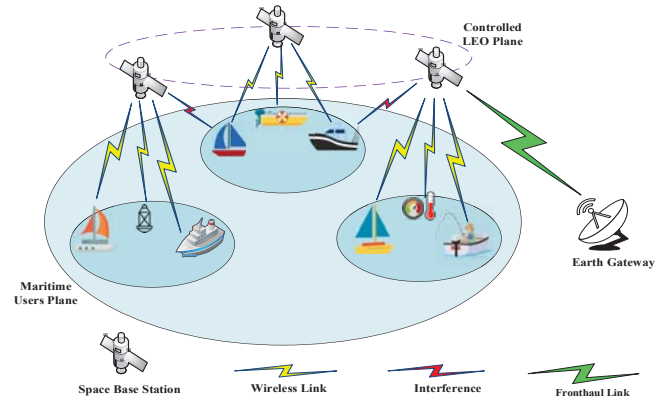


Fig. 1: Illustration of Integrated Space-Oceanic Network

satellite communication and future 6G links. Therefore, we assume that each satellite n and the MUE m are equipped with one antenna, and their large-scale channel effects on the mmW links follow a standard model given as:

$$\delta_{nm} = \omega_{nm} + \rho_{nm} 10 \log_{10} d_{nm} + \psi, \quad (1)$$

where δ_{nm} is denote the pathloss at mmWave frequencies for all MUEs associated with satellite, ρ_{nm} is the slope of the fit (pathloss exponent) and ω_{nm} indicate the intercept parameter, which is the pathloss (dB) for 1 meter of distance, $d_{nm} = \left(\sqrt{(x_n - x_m)^2 + (y_n - y_m)^2 + (h_n - h_m)^2} \right)$ represents the distance between the satellite n and MUE m . Moreover, ψ models the deviation in fitting (dB) which is a Gaussian random variable with zero mean and variance ξ_{nm}^2 for 1 meter of distance. Therefore, the channel model between the satellite n and MUE m can be define as:

$$g_{nm} = \beta_{nm} 10^{-\delta_{nm}/10}, \quad \forall n \in \mathcal{N}, \forall m \in \mathcal{M}, \quad (2)$$

where β_{nm} is the Rician fading channel coefficient, which indicates the small-scale fading between the satellite n and MUE m , this fading is responsible for line-of-sight (LoS) and multi-path scattering, which occurs at each MUE m . Specifically, adopting the Rician channel modeling between the satellite n and MUE m is substantiated by a dominated LoS link between both network nodes. Moreover, we assume that the Doppler effect of mobile MUE can be compensated from the existing frequency synchronization techniques, i.e., phase-locked loop [11]. The signal-to-interference-plus-noise ratio (SINR) γ_{nm} of the satellite n and MUE m can be given as:

$$\gamma_{nm} = \frac{p_{nm} g_{nm}}{I_{nm} + \sigma^2}, \quad (3)$$

where $p_{nm} = \bar{p}_{nm}/k_{nm}$ is the transmission power of satellite n to each MUE m over allocated resource block k_{nm} and \bar{p}_{nm} is the total transmission power of satellite n to MUE m . Moreover, σ^2 denotes the additive white noise power of the associated resource block k which has the bandwidth of b_{nm} . The interference from non-associated satellites to MUE m by transmitting the same resource block k is given by

$I_{nm} = \eta \sum_{\forall n' \neq n} \sum_{\forall m' \neq m} a_{n'm'} p_{n'm'} g_{n'm'}$, where the received power corresponds to the transmit power received by MUE m from the satellite n , the inter-cell interference corresponds to all the received interference from all the others satellites n' , $\forall n' \neq n$. Therefore, the total achievable data rate of satellite n associated with the m MUEs can be defined as:

$$R_{nm}(\mathbf{p}_{nm}) = \sum_{m \in \mathcal{M}} b_{nm} \log_2(1 + \gamma_{nm}). \quad (4)$$

Similarly, a_{nm} indicate the satellite-MUE association which can define as:

$$a_{nm} = \begin{cases} 1, & \text{if MUE } m \in \mathcal{M} \text{ is served by satellite } n \in \mathcal{N}, \\ 0, & \text{otherwise.} \end{cases} \quad (5)$$

Each satellite $n \in \mathcal{N}$ is assigned the same bandwidth denoted by b_n . This bandwidth b_n is further categories equally into associated MUEs i.e., $b_{nm} = \frac{b_n}{\sum_{m \in \mathcal{M}} a_{nm}}$. This divided bandwidth allocate to the communication link between satellite $n \in \mathcal{N}$ and MUE $m \in \mathcal{M}$, where $\sum_{m \in \mathcal{M}} a_{nm}$ indicates all the associated MUEs with the satellite n .

B. Data Transmission & Processing Power Model

We model the power expenditure according to [12], the power expending by each satellite is formulated by two parameters, firstly the data-dependent power of each satellite n can be given as:

$$p_{nm}^d = \sum_{m \in \mathcal{M}} a_{nm} p_{nm}, \quad (6)$$

secondly, independent data power is the expenditure in circuit processing and core network transmission. The power consumed by independent of data in each satellite n is denoted as p_n^{core} . Therefore, the power expenditure model of each satellite n can be formulated as:

$$p_{nm}(\mathbf{a}_{nm}) = p_{nm}^d + p_n^{\text{core}}, \quad (7)$$

for the sake of convenience, we assume the p_n^{core} as a constant term for each satellite n to the core network communication.

IV. PROBLEM FORMULATION

Our objective is to provide the solution to the network profit maximization (NPM) problem, where we need to maximize the weighted sum throughput (sumrate) and minimize each satellite's power expenditure simultaneously. The weighted sumrate and transmit power expenditure can be considered the revenue (income) and cost (outcome) of the maritime network. The optimization goal is to maximize the network profit, which can be expressed as maximize the integrated network total throughput and meanwhile minimize the transmission power under the constraint of SINR and minimum data rate requirement of each MUE m . We can formulate the network profit function for the maximization as follows:

$$f(\mathbf{p}, \mathbf{a}) = \sum_{n \in \mathcal{N}} \sum_{m \in \mathcal{M}} [\gamma_m R_{nm}(\mathbf{p}_{nm}) - \chi p_{nm}(\mathbf{a}_{nm})], \quad (8)$$

where $\mathbf{p} = [p_{nm}] \in \mathcal{R}^{N \times M}$, χ indicate a constant value, which denotes the fraction of revenue per unit sum-rate and cost per unit transmit power, and $\gamma_m \in \mathcal{R}^{1 \times M}$ are the weights of different MUEs. A variable χ is utilized to show the linear relation between sumrate and transmit power expenditure, and χ can be updated at each iteration to increase energy efficiency in the Dinkelbach algorithm (DA) given in [12]. Though (8) represents the linear relationship of the sumrate and transmit power expenditure, the main disagreement of χ is fix valued, in place of the variable given in the DA. Besides, in our case, χ can dynamically be fixed for various network configurations, which intensify the prevalence of the profit measure. This framework analogous to the linear combination structure for multiobjective optimization [13] as well. Therefore, the optimization problem is formulated as:

$$\max_{\mathbf{a}, \mathbf{p}} f(\mathbf{p}, \mathbf{a}), \quad (9a)$$

$$\text{s.t. } \frac{p_{nm} g_{nm}}{I_{nm} + \sigma^2} \geq \Gamma_{nm}, \quad \forall n \in \mathcal{N}, \forall m \in \mathcal{M}, \quad (9b)$$

$$R_{nm}(\mathbf{p}_{nm}) \geq R_{nm}^{\min}, \quad \forall n \in \mathcal{N}, \forall m \in \mathcal{M}, \quad (9c)$$

$$0 \leq \sum_{m \in \mathcal{M}} p_{nm} \leq P_n^{\max}, \quad \forall n \in \mathcal{N}, \quad (9d)$$

$$\sum_{m \in \mathcal{M}} a_{nm} \leq 1, \quad \forall n \in \mathcal{N}, \quad (9e)$$

$$a_{nm} \in \{0, 1\}, \quad \forall n \in \mathcal{N}, \forall m \in \mathcal{M}. \quad (9f)$$

The objective function (9a) is to maximize the network profit based on power allocation and MUE association. In constraint (9b), Γ_{nm} is the minimum SINR requirement of each MUE m to get services from the satellite n . Constraint (9c) means the minimum data transmission rate by each satellite should satisfy for each MUE m . In constraint (9d), P_n^{\max} is the maximum transmit power of each satellite n . Additionally, (9e) and (9f) ensures that MUE can associate at most one satellite at a time. It is difficult to find a unique solution to our optimization problem because it has several association strategies available for NPM. The optimal solution set of a given problem can denote as follows:

$$\Pi^* = \{(\mathbf{a}^*, \mathbf{p}^*) \mid \forall (\mathbf{a}, \mathbf{p})\}, \quad (10)$$

where Π^* is an optimal solution strategy to the given optimization problem. Our goal is to find $(\mathbf{a}^*, \mathbf{p}^*)$, which maximizes the net profit by consuming less amount of power. Therefore, the presented framework will achieve this optimal strategy.

V. GLOBAL OPTIMIZATION ALGORITHM BASED ON BENDER DECOMPOSITION

We propose a joint MUEs association and resource allocation algorithm in this section, which is based on BD and optimization solver. BD is utilized to separate the integer and continuous variables. We use an optimization solver for both the integer and continuous variables problem to solve these problems separately because it solves the problem centrally, suitable for network topology due to remote control of satellite constellation. Therefore, we used BD in the outer loop and

optimization solver in an inner loop, which we describe in the following sections. A network topology implementation and its optimization results are given according to this framework. BD is a famous solution method for MINLP [14]. This algorithm decomposes the MINLP into an integer (binary) linear programming as a master problem and continuous non-linear programming as a subproblem [14]. The master problem objective is to solve the integer linear programming problem, while the subproblem is to solve the continuous programming problem. This algorithm is based on an iterative process that can converge when the desired condition meets. Firstly, the initialization phase occurs for a given problem. Then, the subproblem solves by utilizing only continuous variables due to the fixation of integer variables. By solving the subproblem, the continuous variables solution obtains, and the dual variables associated with fixed integer variables are also obtained. After getting this solution, we generate Bender's cut for feasibility and optimality conditions; thus, the master problem can be solved. Subsequently, the upper and lower bounds difference provides the stopping criterion for this algorithm. The overall process of solving joint MUEs association and power allocation problem is given below:

Initialization: Firstly, we consider the master problem has a trivial solution and can generate the initialization in the given problem. After that, we need to assign the loop counter, i.e., $z = 1$. We have association variable a_{nm} in binary form in our problem formulation. Therefore the upper and the lower bound can denote as $a_{UB} = 1$ and $a_{LB} = 0$ respectively. Moreover, we implement a function ζ as an auxiliary variable, representing the optimal value of the subproblem's objective function within the objective function of the master problem. The initial value for the function $\zeta^{(z)}$ as ζ^{down} , to avoid unbounded solution in the first iteration when no Bender cut is added. Its value can be a huge negative, i.e., -10^6 .

Subproblem: The idea behind subproblem construction is to fix the value of association variables \mathbf{a} to avoid them. Therefore, we can express the subproblem as given in (11). We can represent the dual variable for the constraints that fixed association variables values, i.e., κ_{nm}^z . Hence, the subproblem can be obtained with only power \mathbf{p} (continuous) variables, and it can be represented as:

$$\min_{\mathbf{p}} f_1(\mathbf{p}, \hat{\mathbf{a}}), \quad (11a)$$

$$\text{s.t. } f_1(\mathbf{p}, \hat{\mathbf{a}}) = -\beta_{nm} R_{nm}(\mathbf{p}_{nm}), \quad \forall n \in \mathcal{N}, \forall m \in \mathcal{M}, \quad (11b)$$

$$\frac{p_{nm} g_{nm}}{I_{nm} + \sigma^2} \geq \Gamma_{nm}, \quad \forall n \in \mathcal{N}, \forall m \in \mathcal{M}, \quad (11c)$$

$$R_{nm}(\mathbf{p}_{nm}) \geq R_{nm}^{\min}, \quad \forall n \in \mathcal{N}, \forall m \in \mathcal{M}, \quad (11d)$$

$$0 \leq \sum_{m \in \mathcal{M}} p_{n,m} \leq P_n^{\max}, \quad \forall n \in \mathcal{N}, \quad (11e)$$

$$a_{nm} = a_{nm}^z : \kappa_{nm}^z, \quad \forall n \in \mathcal{N}, \forall m \in \mathcal{M}. \quad (11f)$$

where $\hat{\mathbf{a}}$ are the initialized MUEs association vectors. We can solve the subproblem by optimization solver due to its convex nature. After solving the subproblem, we can obtain the $\hat{\mathbf{p}}_{nm}$

Algorithm 1 Profit Maximization by Bender's Decomposition

- 1: Initialize: loop counter $z = 0$, U_{up} , U_{down} , $\zeta^{(z)}$, ϵ , χ
 - 2: **while** $U_{\text{up}}^{(z)} - U_{\text{down}}^{(z)} > \epsilon$ **do**
 - 3: **Subproblem**
 - 4: obtain $\hat{\mathbf{p}}_{nm}^z$ and κ_{nm}^z , use optimization solver due to convex problem
 - 5: **Bounds calculation**
 - 6: find the both upper and lower bounds ($U_{\text{up}}^{(z)}$ and $U_{\text{down}}^{(z)}$) by (12) and (13)
 - 7: **Master Problem**
 - 8: step 1: increment in loop counter $z = z + 1$
 - 9: step 2: put new Benders cut to problem (15)
 - 10: step 3: solve the updated master problem
 - 11: step 4: acquire the optimal value of $\hat{\mathbf{a}}_{nm}$ and ζ^z
 - 12: **end while**
-

and κ_{nm}^z for solving the following steps.

Convergence Analysis: The algorithm stopping criterion is deduced by checking its convergence, which plays a significant role to stop this iterative algorithm. We can find the upper bound for the master problem as:

$$U_{\text{up}}^{(z)} = f(\hat{\mathbf{p}}, \hat{\mathbf{a}}). \quad (12)$$

Furthermore, the lower bound can be find as:

$$U_{\text{down}}^{(z)} = f_2(\hat{\mathbf{p}}, \mathbf{a}) + \zeta^z. \quad (13)$$

Therefore, the algorithm criterion for stopping can be given as:

$$\begin{cases} U_{\text{up}}^{(z)} - U_{\text{down}}^{(z)} \leq \epsilon, & \text{stop,} \\ \text{otherwise,} & \text{continue,} \end{cases} \quad (14)$$

where tolerance parameter ϵ can be pre-defined. After the convergence of algorithm, optimal value of $\mathbf{a}^{*(z)}$ and $\mathbf{p}^{*(z)}$ can be obtained.

Master Problem: This problem only deals with association variables $\mathbf{a}^{(z)}$ in the network. When the loop counter update as $z = z + 1$, then the following problem need to solve which is:

$$\min_{\mathbf{a}, \zeta} f_2(\hat{\mathbf{p}}, \mathbf{a}) + \zeta, \quad (15a)$$

$$\text{s.t. } f_2(\hat{\mathbf{p}}, \mathbf{a}) = \chi_{nm} \sum_{n \in \mathcal{N}} \sum_{m \in \mathcal{M}} e_{nm}(\mathbf{a}_{nm}), \quad (15b)$$

$$\begin{aligned} \zeta &\geq \hat{\kappa}_{nm}^{zT} (\hat{\mathbf{a}}_{nm} - \hat{\mathbf{a}}_{nm}^z) \\ &\quad - \sum_{n \in \mathcal{N}} \sum_{m \in \mathcal{M}} \beta_{nm} R_{nm}(\hat{\mathbf{p}}_{nm}^z), \quad \forall n, m, \end{aligned} \quad (15c)$$

$$\zeta \geq \zeta^{\text{down}}, \quad (15d)$$

$$\sum_{m \in \mathcal{M}} a_{nm} \leq 1, \quad \forall n \in \mathcal{N}, \quad (15e)$$

$$a_{nm} \in \{0, 1\}, \quad \forall n \in \mathcal{N}, m \in \mathcal{M}. \quad (15f)$$

The inequality constraints in (15c) and (15d) are representing the Bender's optimality and feasibility cuts, respectively, which is associated to the former iterations. Every iteration

TABLE I: Simulation Parameters

Parameters	Values	Parameters	Values
P^{\max}	30 dBm	N_0	-174 dBm/Hz
f	30 GHz	b	20 MHz
Coverage area	500 * 500 NM	area/satellite	250 km ²
χ	5×10^5	R_{min}	10 Mbps
h_{nm}	1.53	P_n^{core}	40 dBm
η	[0, 1]	h_n	200 km

generates a new Benders cut, which will add to the master problem in the form of constraint. The $z - 1$ Benders cuts approximate the subproblem's objective function from below by hyperplanes. By getting the solution of the master problem, a new iteration starts with the subproblem solution. The details of BD is depicted in algorithm 1.

VI. SIMULATION RESULTS AND DISCUSSION

This section provides numerical simulation results of the proposed resource allocation algorithm to evaluate the network profit performance in a space-oceanic network topology. The mmWave carrier frequency is considered from Ka-band, i.e., 27 and 30 GHz due to the long coverage area. The bandwidth b_n of each satellite n is allocated as 20 MHz, which is further distribute among the connected MUEs as resource blocks to reduce interference among the network. Moreover, each satellite utilizes the same bandwidth for the connected MUEs to reuse the frequency spectrum. Similarly, the power of noise to each resource block is the $\sigma_{nm}^2 = b_n/k_{nm} \times N_0$, is the additive white Gaussian noise (AWGN) power spectral density. The channel gain of each satellite-MUE link is assumed LoS, which follows the Rician distribution. The interference in resource block allocation from the non-associated satellite is controlled by the parameter η . The parametric values for stated variables and other constraints are declared in the parameters table I.

Fig. 2 shows the implemented network topology for a given system model. The satellites are considered at the altitude of 200 km from the earth's surface. The number of satellites is considered $n = 3$, and the number of MUE in each satellite coverage region is $m = 10$. Each satellite's coverage radius is considered 250 nautical miles (NM), which is about 463 km. The MUEs are uniformly distributed over a range of 500×500 NM in sea waters. Each MUE is associate at most one satellite-based on less Euclidean distance d_{nm} .

In Fig. 3, the convergence of the BD algorithm is presented. The value of a master problem and subproblem is U_{up} and U_{down} respectively. As shown in Fig. 3, the value of the master problem remains higher, and the value of the subproblem remain lower than the optimal value till convergence. Moreover, the BD algorithm converges about thirty-two iterations, which are quite good.

In the upper part of Fig. 4, we show the overall network utility of all the satellites with various MUEs associations in the network by keeping all the variable settings as previous. We observe by increasing the number of MUEs association from 5 to 50; the overall network utility increases from 700 Mbps

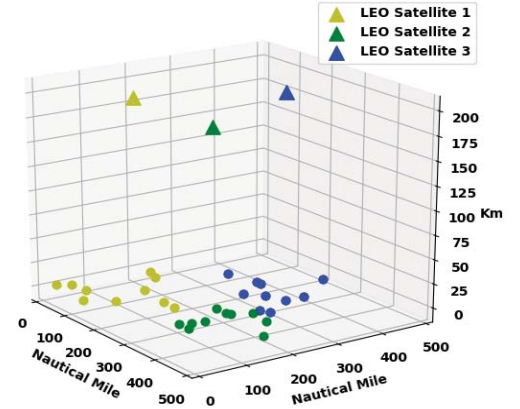


Fig. 2: Oceanic-Space Network Topology

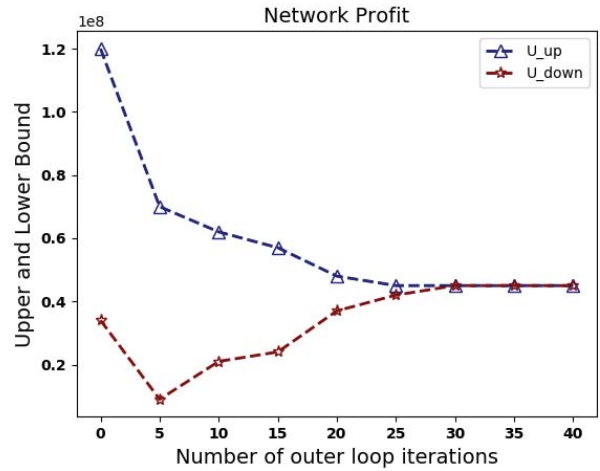


Fig. 3: Bender decomposition convergence performance

to 850 Mbps when the carrier frequency $f = 30$ GHz. Similarly, this trend remains the same for the carrier frequency $f = 27$ GHz with a 0.5 % increase. The one interesting pattern of results is when the sub-6 GHz band is utilized as a carrier frequency, which increases network utility about 9 %, due to less pathloss.

In the lower part of Fig. 4, it represents the effect of bandwidth on the overall network utility of all the satellites. We keep all the variables constant and study BW's trend from 10 MHz to 20 MHz; the incremental BW in the network enhances the total utility by varying the number of MUEs association from 5 to 50. When $BW = 10$ MHz, the network utility increases from 370 MHz to 470 MHz with MUEs association from 5 to 50. Similarly, when $BW = 15$ MHz, the network utility increases from 530 MHz to 680 MHz. Therefore, the broad BW spectrum can reach maximum network utility when the carrier frequency remains the same

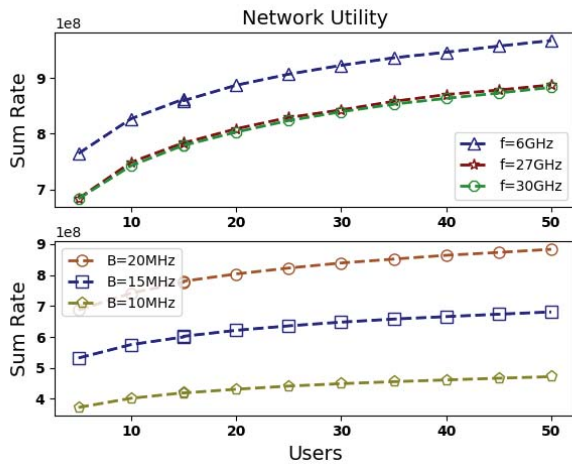


Fig. 4: Network Sumrate vs Users

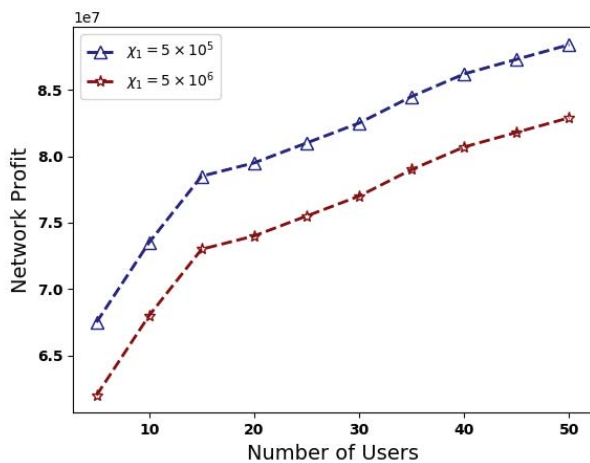


Fig. 5: Network Profit and χ Relation

at Ka-band, i.e., 30 GHz. Thus, our proposed algorithm can provide high network utility in the oceanic-space network.

We present the importance of χ in different network configurations. In Fig. 5, the network profit exhibits more value when $\chi = 5 \times 10^5$ as compared to $\chi = 5 \times 10^6$. As previously mentioned, this value depends on the fraction of network profit per unit datarate and the expenditure per unit transmission power. The increment in χ value directly affects the power consumption in this scenario. Therefore, network profits decrease when the value of χ increases.

VII. CONCLUSION

In this paper, we proposed the framework of the next-generation network architecture of marine user's communication. We analyzed the satellite's MUE association and resource allocation scheme and provided the network profit in utility and power consumption terms. We formulated an optimization problem of profit maximization, which was mixed integer nonlinear programming. We solved the optimization problem

by utilizing the Bender decomposition approach, which is the best fit for integer variables, and proposed an algorithm for the optimal association and power resource allocation from the satellites. Numerical results demonstrate that our proposed framework converges to an optimal value. Moreover, the proposed algorithm has provided good results for different cases. We will consider network nodes' mobility in future work, i.e., satellites and marine users, during association and resource allocation.

REFERENCES

- [1] L. U. Khan, I. Yaqoob, M. Imran, Z. Han, and C. S. Hong, "6G wireless systems: A vision, architectural elements, and future directions," *IEEE Access*, vol. 8, pp. 147 029–147 044, 2020.
- [2] Y. M. Dai and K. S. Liu, "TACSA: A web-service based system for coastal surveillance and situational awareness," in *Proc. of the International Carnahan Conference on Security Technology (ICCS)*, Taipei, Taiwan, September 2015, pp. 409–413.
- [3] J. Wozniak, K. Gierlowski, and M. Hoefl, "Broadband communication solutions for maritime ITSs: Wider and faster deployment of new e-navigation services," in *Proc. of the International Conference on ITS Telecommunications (ITST)*, Warsaw, Poland, May 2017, pp. 1–11.
- [4] Y. Su, Y. Liu, Y. Zhou, J. Yuan, H. Cao, and J. Shi, "Broadband LEO satellite communications: Architectures and key technologies," *IEEE Wireless Communications*, vol. 26, no. 2, pp. 55–61, 2019.
- [5] Q. Bi, "Ten trends in the cellular industry and an outlook on 6G," *IEEE Communications Magazine*, vol. 57, no. 12, pp. 31–36, December 2019.
- [6] Q. Zhuang and C. Zheng, "Research on INMARSAT based on Ka band and applications," in *Proc. of the International Conference on Information, Cybernetics and Computational Social Systems (ICCS)*, Dalian, China, July 2017, pp. 127–129.
- [7] J. Mashino, K. Tateishi, K. Muraoka, D. Kurita, S. Suyama, and Y. Kishiyama, "Maritime 5G experiment in windsurfing world cup by using 28 GHz band massive MIMO," in *Proc. of the IEEE Annual International Symposium on Personal, Indoor and Mobile Radio Communications (PIMRC)*, Bologna, Italy, September 2018, pp. 1134–1135.
- [8] S. Jo and W. Shim, "LTE-maritime: High-speed maritime wireless communication based on LTE technology," *IEEE Access*, vol. 7, pp. 53 172–53 181, April 2019.
- [9] Y. Li, L. Su, T. Wei, Z. Zhou, and N. Ge, "Location-aware dynamic beam scheduling for maritime communication systems," in *Proc. of the International Conference on Communications, Circuits and Systems (ICCCAS)*, Chengdu, China, December 2018, pp. 265–268.
- [10] B. Soret, I. Leyva-Mayorga, M. Röper, D. Wübben, B. Matthiesen, A. Dekorsy, and P. Popovski, "LEO small-satellite constellations for 5G and beyond-5G communications," *arXiv preprint arXiv:1912.08110*, 2019.
- [11] Y. Zeng and R. Zhang, "Energy-efficient UAV communication with trajectory optimization," *IEEE Transactions on Wireless Communications*, vol. 16, no. 6, pp. 3747–3760, 2017.
- [12] Z. Wu, Z. Fei, Y. Yu, and Z. Han, "Toward optimal remote radio head activation, user association, and power allocation in C-RANs using Benders decomposition and ADMM," *IEEE Transactions on Communications*, vol. 67, no. 7, pp. 5008–5023, 2019.
- [13] Z. Fei, B. Li, S. Yang, C. Xing, H. Chen, and L. Hanzo, "A survey of multi-objective optimization in wireless sensor networks: Metrics, algorithms, and open problems," *IEEE Communications Surveys Tutorials*, vol. 19, no. 1, pp. 550–586, 2017.
- [14] A. J. Conejo, E. Castillo, R. Minguez, and R. Garcia-Bertrand, *Decomposition techniques in mathematical programming: engineering and science applications*. Springer Science & Business Media, 2006.